Electromagnetic Coupling between Two Half-Space Regions Separated by Two Slot-Perforated Parallel Conducting Screens

YEHUDA LEVIATAN, MEMBER, IEEE

Abstract—**The problem of electromagnetic coupling between two half-space regions separated by two slot-perforated parallel conducting planes is investigated. A general moment solution for the problem is obtained. This moment solution is then specialized to the case of narrow slots and to a TE (transverse electric to the slot axis) excitation. Attention is given to the power transmitted from one half-space to the other through the slots and to its functional dependence on various problem parameters involved.**

I. Introduction

THE PROBLEM OF coupling between regions via apertures and slots in conducting walls has been the subject of interest to researchers for many years. Problems of this nature arise in many practical situations in EMP studies and in the areas of electromagnetic compatability and interference [1]. Another application field is microscopy, where superresolution based upon near-field imaging is investigated [2], [3]. Once extended into the visible frequency regime, this technique will give birth to enormous practical applications. For example, this technique is likely to permit nondestructive imaging of surfaces for use in biophysical research with a resolution comparable to that of scanning electron microscopy. Finally, in the area of microfabrication, the near-field behavior in the vicinity of a photolithographic mask is of unquestionable importance to engineers designing ever smaller devices.

In this paper attention is focused on the problem of electromagnetic coupling between two half-space regions separated by two slot-perforated parallel conducting planes. We specialize our discussion to the case of electrically narrow slots which can be of particular relevance to the areas of microscopy and microfabrication. For example, it would permit an assessment of the power transmission pattern that is expected to result when one moves a narrow slot along an adjacent opaque test object carrying a pattern of fine transparent lines. This problem clearly falls into the general classification of problems with three regions [4]–[8]. We will thus follow a formulation procedure similar to [8].

Manuscript received June 19, 1987; revised August 14, 1987.

The author is with the Department of Electrical Engineering, Technion—Israel Institute of Technology, Haifa 32000, Israel.

IEEE Log Number 8717589.

The basic approach is to first use the equivalence principle [9, sec. 3-5] to divide the problem into three equivalent situations. We close each slot with a perfect conductor and attach magnetic current sheets to both sides of the covered slot to provide for the tangential electric field originally present in the slot region. Subsequently, we require the continuity of the tangential magnetic field across each slot and readily arrive at the functional equations for the problem. These equations are in turn reduced to matrix form via the method of moments, where the various constituents are interpreted in terms of generalized network parameters [10], [11].

For narrow slots, the equivalent magnetic current in each slot can be expanded, in general, in terms of the four quasi-static distributions. While these distributions apply specifically to the canonical problem of a narrow slot in a plane screen, we assume that the *form* of the field in each slot in our case remains almost the same as in the canonical problem. The amplitude and the phase of each slot field, however, would not remain the same. In other words, as far as the form of each slot field is concerned, we neglected the electromagnetic interaction between the two slotted screens, but for calculating its amplitude and phase, we fully take these interactions into account.

Representative numerical simulations of transmitted power patterns as functions of the various geometrical parameters are given in the numerical results section. Associated interpretations are suggested and major conclusions are summarized thereafter.

II. Formulation of the Problem

The geometry of the problem under study is shown in Fig. 1, together with the coordinate system used. Here, we consider the coupling between two half-space regions separated by two slotted parallel-plane conducting screens. The left screen is in the $z = 0$ plane. The right screen is in the $z = d$ plane. The left-hand half-space ($z < 0$) is called region a, the region between the screens is called region b. The boundary condition at $x = +\infty$ and $x = -\infty$ in region b is the radiation condition. The right-hand half-space ($z > d$) is called region c. The slot connecting regions a and b is called slot S_1. The slot is infinite in the y

0018-9480/88/0100-0044$01.00

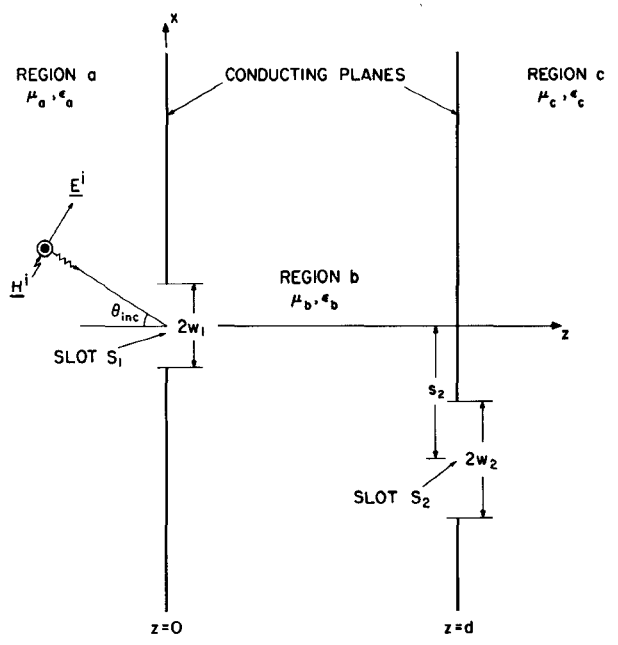

Fig. 1. TE oblique incidence upon the slotted structure.

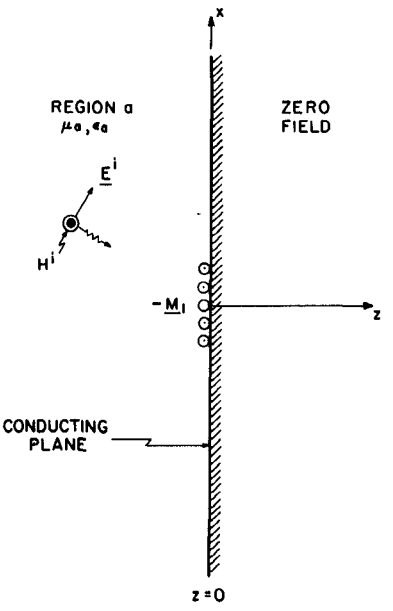

Fig. 2. Equivalence for region a.

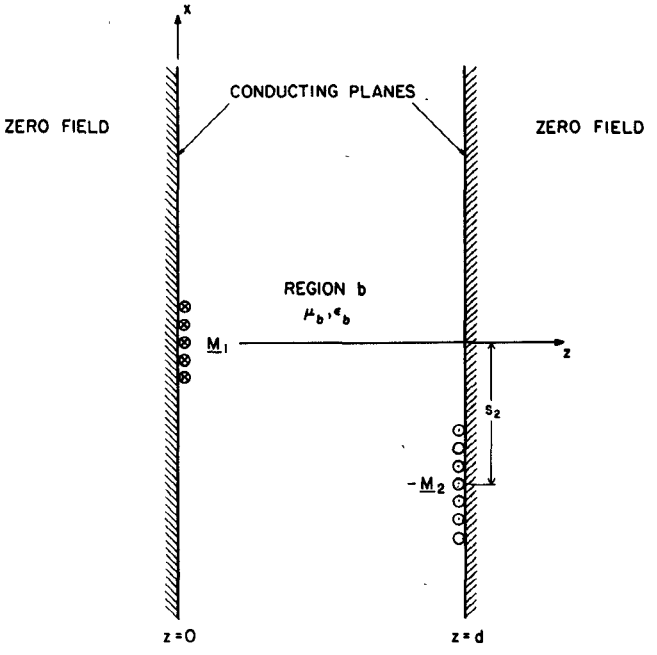

Fig. 3. Equivalence for region b.

direction, or width $2w_1$ in the x direction, and centered at $x = s_1 = 0$. The slot connecting regions b and c is called slot S_2. The slot is infinite in the y direction of width $2w_2$ in the x direction, and centered at $x = s_2$. Regions a, b, and c are each filled with homogeneous media of constitutive parameters (μ_a, ϵ_a), (μ_b, ϵ_b), and (μ_c, ϵ_c), respectively. We are not considering dissipation and, therefore, each μ and each ϵ is real. The excitation is assumed to be due to known y-independent electric and magnetic current sources in region a with $\exp(j\omega t)$ time dependence. Further, it is assumed that throughout the entire frequency range considered, the width of each slot is much smaller than the wavelength.

The equivalence principle is used to divide the original problem into three equivalent situations, as shown in Figs. 2–4. We close the slots with perfect conductors and provide for the electric fields originally present in the slots S_1 and S_2 by attaching postulated magnetic current sheets $-\boldsymbol{M}_1$ and $\boldsymbol{M}_1$ just to the left and right of S_1, respectively, and $-\boldsymbol{M}_2$ and $\boldsymbol{M}_2$ just to the left and right of S_2, respectively. Here,

$$\boldsymbol{M}_1 = \boldsymbol{E}_1 \times \hat{z} \tag{1}$$

$$\boldsymbol{M}_2 = \boldsymbol{E}_2 \times \hat{z} \tag{2}$$

where $\hat{z}$ is a unit vector in the z direction and $\boldsymbol{E}_1$ and $\boldsymbol{E}_2$ are the respective electric fields in S_1 and S_2 in the original problem. The electromagnetic field in region a in Fig. 2 is the sum of the electromagnetic fields of the incident wave $(\boldsymbol{E}^{sc}, \boldsymbol{H}^{sc})$ calculated with slot S_1 shorted and the electromagnetic field $(\boldsymbol{E}^a(-\boldsymbol{M}_1), \boldsymbol{H}^a(-\boldsymbol{M}_1))$ due to $-\boldsymbol{M}_1$ radiating in region a with slot S_1 shorted. The electromagnetic field in region b in Fig. 3 is the electromagnetic field $(\boldsymbol{E}^b(\boldsymbol{M}_1) + \boldsymbol{E}^b(-\boldsymbol{M}_2), \boldsymbol{H}^b(\boldsymbol{M}_1) + \boldsymbol{H}^b(-\boldsymbol{M}_2))$ due to $\boldsymbol{M}_1$ and $-\boldsymbol{M}_2$ radiating in region b with both slots S_1 and S_2 shorted. The electromagnetic field in region c in Fig. 4 is the electromagnetic field $(\boldsymbol{E}^c(\boldsymbol{M}_2), \boldsymbol{H}^c(\boldsymbol{M}_2))$ due to $\boldsymbol{M}_2$ radiating in region c with slot S_2 shorted. These electromagnetic fields simulate the respective fields in regions a, b, and c in the original situation shown in Fig. 1.

The use of $-\boldsymbol{M}_1$ in region a and $\boldsymbol{M}_1$ in region b ensures continuity of the tangential components of the electric field across the slot S_1. The use of $-\boldsymbol{M}_2$ in region b and $\boldsymbol{M}_2$ in region c ensures continuity of the tangential components of the electric field across the slot S_2. Continuity of the tangential components of $\boldsymbol{H}$ across each slot leads to the operator equations for the problem. The

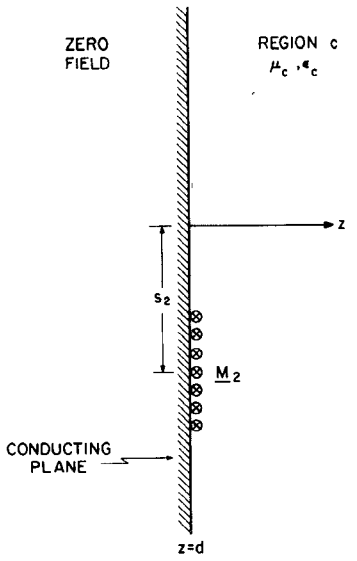

Fig. 4. Equivalence for region c.

procedure is described in detail in [8]. The result is

$$-\boldsymbol{H}_t^a(\boldsymbol{M}_1)-\boldsymbol{H}_t^b(\boldsymbol{M}_1)+\boldsymbol{H}_t^b(\boldsymbol{M}_2)=-\boldsymbol{H}_t^{\mathrm{sc}} \qquad \text{over } S_1 \tag{3}$$

$$\boldsymbol{H}_t^b(\boldsymbol{M}_1)-\boldsymbol{H}_t^b(\boldsymbol{M}_2)-\boldsymbol{H}_t^c(\boldsymbol{M}_2)=0 \qquad \text{over } S_1 \tag{4}$$

where the subscript t denotes components tangential to the respective slot region. Note that in (3) and (4) we have used the linearity of the operator to replace $\boldsymbol{H}_t^a(-\boldsymbol{M}_1)$ and $\boldsymbol{H}_t^b(-\boldsymbol{M}_2)$ by $-\boldsymbol{H}_t^a(\boldsymbol{M}_1)$ and $-\boldsymbol{H}_t^b(\boldsymbol{M}_2)$, respectively. Equations (3) and (4) should be first solved for the equivalent magnetic currents $\boldsymbol{M}_1$ and $\boldsymbol{M}_2$, and then the fields in each region can be computed from these equivalent currents.

If (3) and (4) were satisfied exactly, we would have the true solution. To obtain an approximate solution, we follow a moment procedure similar to that summarized in [8], specializing it to electrically narrow slots [12]. First, the two magnetic currents are expanded as

$$\boldsymbol{M}_q=\sum_{n=1}^{4} V_{qn}\boldsymbol{M}_{qn}, \qquad q=1,2 \tag{5}$$

where the V_{qn} are scalar coefficients to be determined and $\boldsymbol{M}_{qn}$ are vector functions defined in slot S_q as follows:

$$\left.\begin{aligned}
\boldsymbol{M}_{q1}&=f_q^{-1}(x)\,\hat{\boldsymbol{y}} && (6)\\
\boldsymbol{M}_{q2}&=(x-s_q)f_q^{-1}(x)\,\hat{\boldsymbol{y}} && (7)\\
\boldsymbol{M}_{q3}&=f_q(x)\,\hat{\boldsymbol{x}} && (8)\\
\boldsymbol{M}_{q4}&=(x-s_q)f_q(x)\,\hat{\boldsymbol{x}} && (9)
\end{aligned}\right\} \quad q=1,2.$$

Here,

$$f_q(x)=\sqrt{w_q^2-(x-s_q)^2}, \qquad q=1,2 \tag{10}$$

where s_q is the x coordinate of the center of slot S_q and $\hat{\boldsymbol{x}}$ and $\hat{\boldsymbol{y}}$ are unit vectors in the x and y directions, respectively. Recall that for convenience we have chosen $s_1=0$. Next, inner products for each slot are defined as

$$\langle \boldsymbol{A},\boldsymbol{B}\rangle_q=\int_{s_q-w_q}^{s_q+w_q}\boldsymbol{A}\cdot\boldsymbol{B}\,dx, \qquad q=1,2 \tag{11}$$

where the integration is along the x direction in slot S_q. Finally, sets of testing functions $\{\boldsymbol{W}_{qn}\}$ are defined in each S_q, $q=1,2$. With these definitions at hand, (5) is substituted into (3) and (4), which in turn are tested, respectively, with each element of $\{\boldsymbol{W}_{1n}\}$ and with each element of $\{\boldsymbol{W}_{2n}\}$ using (11).

The result is

$$[Y_{11}^a]\vec{V}_1+[Y_{11}^b]\vec{V}_1+[Y_{12}^b]\vec{V}_2=\vec{I}^i \tag{12}$$

$$[Y_{21}^b]\vec{V}_1+[Y_{22}^b]\vec{V}_2+[Y_{22}^c]\vec{V}_2=\vec{0} \tag{13}$$

where

$$[Y_{qq}^p]=\left[-\langle \boldsymbol{W}_{qm},\boldsymbol{H}_t^p(\boldsymbol{M}_{qn})\rangle_q\right] \tag{14}$$

$$[Y_{qr}^b]=\left[\langle \boldsymbol{W}_{qm},\boldsymbol{H}_t^b(\boldsymbol{M}_{rn})\rangle_q\right], \qquad q\neq r \tag{15}$$

$$\vec{I}^i=\left[-\langle \boldsymbol{W}_{1m},\boldsymbol{H}_t^{\mathrm{sc}}\rangle_1\right] \tag{16}$$

$$\vec{V}_q=[V_{qn}] \tag{17}$$

with $q=1,2$ and $r=1,2$. The matrices $[Y_{qr}^p]$ are called generalized admittances, the vector $\vec{I}^i$ is called generalized source current, and the vectors $\vec{V}_q$ are called generalized voltages. A solution of the problem is obtained by solving matrix equations (12) and (13) for $\vec{V}_1$ and $\vec{V}_2$, which determine the equivalent magnetic currents $\boldsymbol{M}_1$ and $\boldsymbol{M}_2$ by (5). If a Galerkin solution is used, that is, if $\{\boldsymbol{W}_{1n}\}=\{\boldsymbol{M}_{1n}\}$ and $\{\boldsymbol{W}_{2n}\}=\{\boldsymbol{M}_{2n}\}$, it then follows that

$$[Y_{qq}^p]=\left[-\langle \boldsymbol{M}_{qm},\boldsymbol{H}_t^p(\boldsymbol{M}_{qn})\rangle_q\right] \tag{18}$$

$$[Y_{qr}^b]=\left[\langle \boldsymbol{M}_{qm},\boldsymbol{H}_t^b(\boldsymbol{M}_{rn})\rangle_q\right], \qquad q\neq r \tag{19}$$

$$\vec{I}^i=\left[-\langle \boldsymbol{M}_{1m},\boldsymbol{H}_t^{\mathrm{sc}}\rangle_1\right]. \tag{20}$$

III. TE Excitation

We here specialize our solution to the case of a TE (transverse electric to the slot axis) illumination. Consider a plane wave incident upon the structure at some angle θ_{inc} in the x–z plane measured from the negative z axis, as shown in Fig. 1. The impressed magnetic field measured in region a in the presence of a complete conducting plane over the $z=0$ plane is

$$\boldsymbol{H}^{\mathrm{sc}}=2H_0\cos(k_a z\cos\theta_{\mathrm{inc}})e^{jk_a x\sin\theta_{\mathrm{inc}}}\hat{\boldsymbol{y}} \tag{21}$$

where H_0 is the amplitude of the incident magnetic field, and k is the wavenumber. The subscript with k associates the wavenumber with its respective region. In view of the excitation, our approximate solution will be basically a one-term moment solution. Specifically, each $\boldsymbol{M}_q$, $q=1,2$, is expressed as

$$\boldsymbol{M}_q=V_{q1}\boldsymbol{M}_{q1} \tag{22}$$

where $\boldsymbol{M}_{q1}$ is given in (6). Using a Galerkin procedure, the general network equations (12) and (13) reduce to the

scalar equations

$$Y_{11}^{a1}V_{11}+Y_{11}^{b1}V_{11}+Y_{12}^{b1}V_{21}=I_1^i \tag{23}$$

$$Y_{21}^{b1}V_{11}+Y_{22}^{b1}V_{21}+Y_{22}^{c1}V_{21}=0. \tag{24}$$

Here, I_1^i is the $m=1$ element of $\vec{I}^i$ and Y_{qr}^{p1} denotes the $(m,n)=(1,1)$ elements of $[Y_{qr}^{p}]$. Further, thanks to reciprocity, we find that $Y_{12}^{b1}=Y_{21}^{b1}$; hence (23) and (24) are equations which characterize the behavior of the equivalent circuit illustrated in Fig. 5.

We next proceed to evaluate the various generalized network parameters appearing in (23) and (24). Substitution of $\boldsymbol{M}_{11}$ from (6) and $\boldsymbol{H}_t^{sc}$ from (21) into (20) and utilizing the fact that $\boldsymbol{H}_t^{sc}$ is virtually constant in the electrically narrow region of slot S_1, we obtain

$$I_1^i=-2\pi H_0. \tag{25}$$

Note that under our assumptions I_1^i is independent of θ_{inc}. Further, following the derivations outlined in the Appendix, the generalized admittances are given by

$$Y_{11}^{a1}=\frac{k_a\pi^2}{2\eta_a}-j\frac{k_a\pi}{\eta_a}\log\left(\frac{\gamma k_a w_1}{4}\right) \tag{26}$$

$$\begin{aligned}Y_{11}^{b1}=&\frac{k_b\pi^2}{2\eta_b}-j\frac{k_b\pi}{\eta_b}\log\left(\frac{\gamma k_b w_1}{4}\right)\\&+\frac{k_b}{\eta_b}\sum_{n=1}^{N_1}\int_{-w_1}^{w_1}\int_{-w_1}^{w_1}\frac{1}{\sqrt{w_1^2-x'^2}}\frac{1}{\sqrt{w_1^2-x^2}}\\&\cdot H_0^{(2)}\left(k_b\sqrt{(2nd)^2+(x-x')^2}\right)dx'dx\\&+\frac{k_b\pi^2}{\eta_b}\sum_{n=N_1+1}^{\infty}H_0^{(2)}(2k_bnd)\end{aligned} \tag{27}$$

$$\begin{aligned}Y_{21}^{b1}=Y_{12}^{b1}=&-\frac{k_b}{\eta_b}\\&\cdot\sum_{n=1}^{N_2}\int_{-w_1}^{w_1}\int_{s_2-w_2}^{s_2+w_2}\frac{1}{\sqrt{w_2^2-(x'-s_2)^2}}\frac{1}{\sqrt{w_1^2-x^2}}\\&\cdot H_0^{(2)}\left(k_b\sqrt{[(2n-1)d]^2+(x-x')^2}\right)dx'dx\\&-\frac{k_b\pi^2}{\eta_b}\sum_{n=N_2+1}^{\infty}H_0^{(2)}\left(k_b\sqrt{[(2n-1)d]^2+s_2^2}\right)\end{aligned} \tag{28}$$

$$\begin{aligned}Y_{22}^{b1}=&\frac{k_b\pi^2}{2\eta_b}-j\frac{k_b\pi}{\eta_b}\log\left(\frac{\gamma k_b w_2}{4}\right)\\&+\frac{k_b}{\eta_b}\sum_{n=1}^{N_1}\int_{-w_2}^{w_2}\int_{-w_2}^{w_2}\frac{1}{\sqrt{w_2^2-x'^2}}\frac{1}{\sqrt{w_2^2-x^2}}\\&\cdot H_0^{(2)}\left(k_b\sqrt{(2nd)^2+(x-x')^2}\right)dx'dx\\&+\frac{k_b\pi^2}{\eta_b}\sum_{n=N_1+1}^{\infty}H_0^{(2)}(2k_bnd)\end{aligned} \tag{29}$$

$$Y_{22}^{c1}=\frac{k_c\pi^2}{2\eta_c}-j\frac{k_c\pi}{\eta_c}\log\left(\frac{\gamma k_c w_2}{4}\right). \tag{30}$$

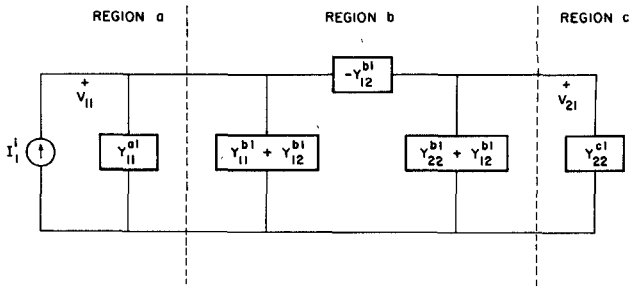

Fig. 5. Equivalent circuit for the coupling between the slotted screens.

The notations of (26)–(30) are also introduced in the Appendix. This completes the evaluation of the various generalized network parameters appearing in (23) and (24).

A parameter of interest is the transfer admittance

$$Y_{12}=\frac{I_1^i}{V_{21}}=\frac{Y_{12}^{b1}Y_{21}^{b1}-\left(Y_{11}^{a1}+Y_{11}^{b1}\right)\left(Y_{22}^{b1}+Y_{22}^{c1}\right)}{Y_{21}^{b1}} \tag{31}$$

which allows one to calculate the strength of $\boldsymbol{M}_2=V_{21}\boldsymbol{M}_{21}$ given the excitation I_1^i of (25). Another measurement of considerable interest is the power transmitted through the two slots to region c. In terms of the above generalized network parameters, this transmitted power is equal to the power dissipated in Y_{22}^{c1} of the equivalent circuit of Fig. 5, that is,

$$P_{trans}=|V_{21}|^2G_{22}^{c1}. \tag{32}$$

In terms of the transfer admittance, this becomes

$$P_{trans}=\left|\frac{I_1^i}{Y_{12}}\right|^2G_{22}^{c1} \tag{33}$$

where I_1^i is given by (25), Y_{12} by (31), and $G_{22}^{c1}=\mathrm{Re}(Y_{22}^{c1})$, with Y_{22}^{c1} given by (30).

The power per unit length is the y direction incident upon the slot S_1 when the incidence is normal is

$$P_{inc}^n=\eta_a|H_0|^2w_1 \tag{34}$$

where the superscript n indicates that the power defined here is for normal incidence. We can now define the transmission coefficient T of the system to be the power transmitted through the slots to region c normalized with respect to the incident power (34), that is,

$$T=\frac{P_{trans}}{P_{inc}^n}. \tag{35}$$

The transmission coefficient is a suitable measure for the power coupling mechanism between regions a and c. It depends on the slot widths, the spacing between the screens, the transverse shift between the slots, and the media filling the various regions. This definition of T has been used in [6] and [8]. It should be distinguished from another possible transmission measure, defined as the power transmitted to region c normalized with respect to the actual power transmitted by slot S_1. This latter quantity would be, of course, smaller than or equal to 1. T of (35), however, can be larger than 1. In the following section,

representative variations of T as functions of various geometrical parameters will be discussed.

IV. Numerical Results

Computer programs have been prepared to carry out the analysis of the preceding section. The programs compute the transmission from region a to region c through the two slotted screens for various slot widths, for various spacings between the screens, and for various transverse shiftings between the slots. All the calculations were done using an IBM 3081 computer. Attention should be recalled to the summations in (27)–(29). Unfortunately, these summations converge slowly, particularly when the spacing between the screens is small, thereby taxing the computing system. Nevertheless, the overall computation time was reasonable. In this section, representative numerical results of transmitted power patterns as function of geometrical parameters are exhibited, and associated interpretations are suggested. It should also be added that the geometry in Fig. 1 is only a representative one. The slot widths can in some cases be larger while in other cases smaller compared with the screen spacing.

Figs. 6 and 7 show plots of transmission coefficient T versus s_2/λ for various screen spacings d. Here, $w_1 = 0.05\lambda$ and $w_2 = 0.1\lambda$, and we take the media in all three regions to be free space. λ is the wavelength in free space. The excitation is due to a plane wave transverse electric to the left slot axis obliquely incident upon the left screen. Fig. 6 depicts the variation in T in the range $-0.3\lambda \leqslant s_2 \leqslant 0.3\lambda$. Fig. 7 is a three-dimensional picture of the data displayed in Fig. 6. An examination of these plots brings out a number of interesting observations. For small distances between the screens, namely, out to about half the first slot width, a distance to which the radiation emanating through the first slot is collimated to the slot size rather than the wavelength [13], a scan of slot S_2 in the x direction yields an approximate scan trace of S_2 in the power transmission coefficient. The smooth edges are of the order of the width of the illuminating slot S_1. In other words, as long as the scan in the x direction is less than $w_2 - w_1$, namely, $|s_2| < 0.05\lambda$, the well-collimated radiation from slot S_1 goes almost unaffected through S_2. As $|s_2|$ increases from 0.05λ, there is a monotonic decline in power transmission, since slot S_2 begins to block this collimated radiation. On the other hand, for larger distances between the screens, the radiation from S_1 is no longer confined to a region comparable with the slot width; consequently, a scan of slot S_2 in the x direction does not yield a well-defined trace of S_2.

Fig. 8 shows a plot of transmission coefficient T at $d = 0.04\lambda$ and $d = 0.1\lambda$ versus s_2/λ for a wide range of s_2 in the x direction, namely, $-2\lambda \leqslant s_2 \leqslant 2\lambda$. Here, $w_1 = 0.05\lambda$ and $w_2 = 0.1\lambda$. Note that T becomes a maximum at transverse shifts that approach multiples of $\lambda/2$ in addition to its maximum at zero offset. This feature seems to cast a severe drawback for scanning ultramicroscopy and photolithography. Fortunately, this problem can be easily overcome by utilizing a multiple-frequency source, thereby significantly enhancing the desired zero offset resonance

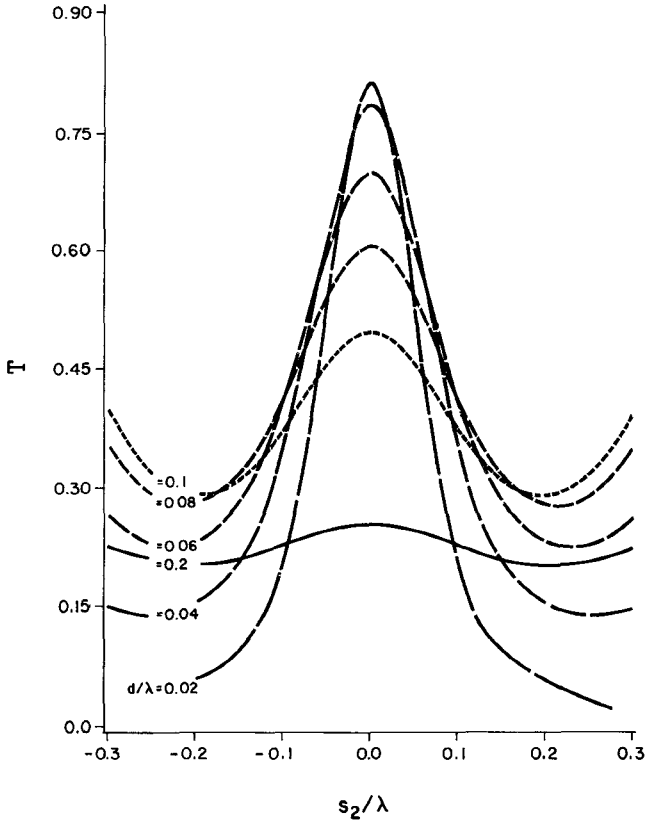

Fig. 6. Plots of transmission coefficient T versus s_2/λ for different spacings between screens.

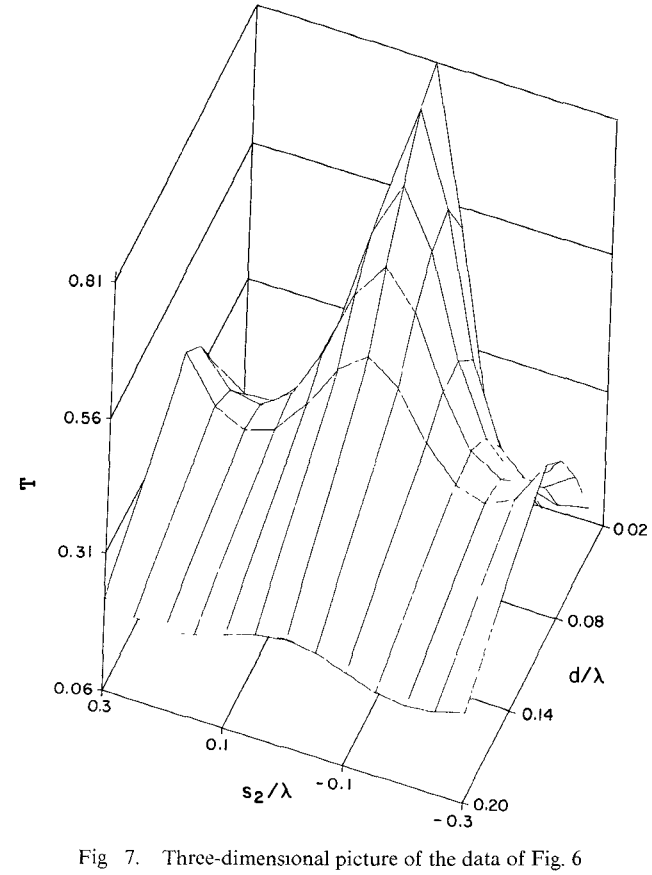

Fig. 7. Three-dimensional picture of the data of Fig. 6

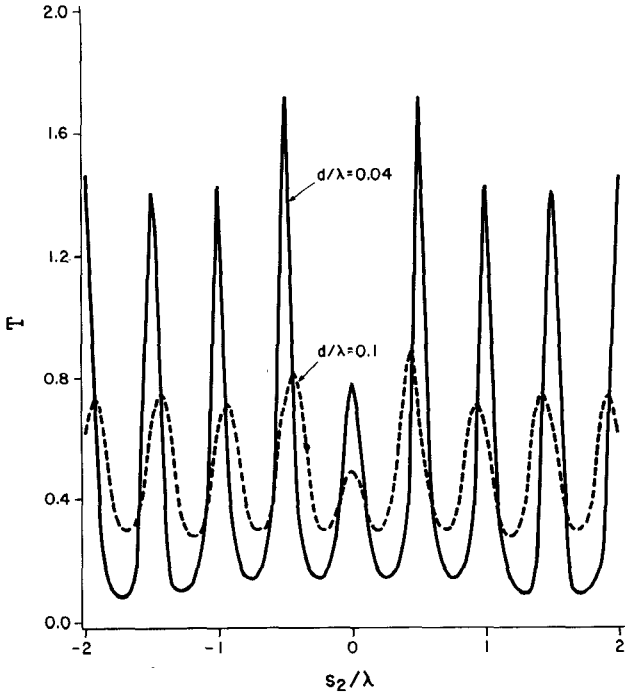

Fig. 8. Transmission coefficient T versus s_2/λ at $d = 0.04\lambda$ and $d = 0.1\lambda$.

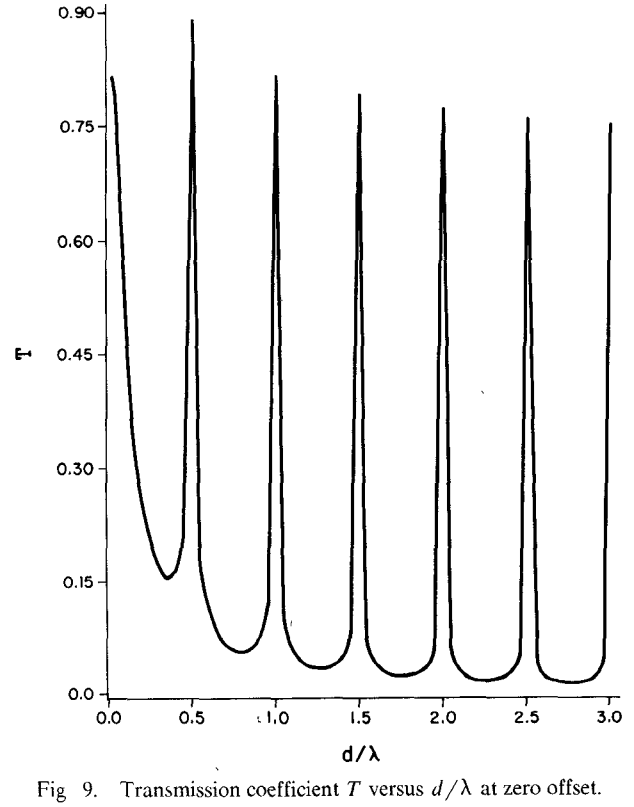

Fig 9. Transmission coefficient T versus d/λ at zero offset.

while retaining the other resonances virtually the same. Observe also that, as one can expect, the resonances become broader and decrease in intensity as d gets larger.

Finally, Fig. 9 depicts a plot of the transmission coefficient T as a function of the spacing between the screens for the zero offset case ($s_2 = 0$). Note that resonances occur at spacings which approach multiples of $\lambda/2$. This phenomenon is not surprising since it has already been observed in similar but nevertheless different situations. These analogous cases are transmission through aperture-cavity-aperture system [8] and transmission through various slots in thick conducting screens [6]. These resonances decrease gradually in intensity, of course, with increasing spacing between the screens.

V. Discussion

A four-term moment solution for the general problem of electromagnetic coupling between two half-space regions separated by two narrow-slot perforated parallel conducting planes has been formulated. The solution reduces subsequently to a one-term one for the special case of TE excitation, where the coupling mechanism is described by means of a simple equivalent circuit model. A measurement of the coupling is given in terms of a transmission coefficient which is defined as the power transmitted through the slots to region c normalized to the power incident upon slot S_1.

The formulation is general and can be employed in a variety of situations involving coupling through slotted screens. Our numerical examples are also general but, in a sense, more closely related to the areas of microscopy and microfabrication. It has been shown that for small distances between the screens, namely, out to about half the first slot width, a scan of the second slot in the transverse direction yields an approximated scan trace of this slot in the power transmission coefficient.

Also, scanning further out along the transverse direction results in a series of power transmission resonances which occur at transverse shifts that approach multiples of $\lambda/2$. We would like to stress again that this behavior, which at first sight seems to cast a severe drawback for scanning ultramicroscopy and photolithography, can be easily overcome by utilizing a multiple-frequency source, thereby significantly enhancing the desired zero offset resonance while retaining the other resonances virtually the same. Furthermore, it should be emphasized that for superresolution fluorescence near-field scanning microscopy, this problem does not exist at all due to the inherently wide spectral content of the fluorescence.

Finally, spacing the screen further apart also leads to a multiple resonance pattern for the zero offset case. These resonances also occur at resonance spacings which approach, as expected, multiples of $\lambda/2$. This last phenomenon is analogous to the phenomenon of transmission through aperture-cavity-aperture system [8] and to that of transmission through narrow slots in thick conducting screens [6], where periodic resonance patterns have already been observed.

Appendix

In this appendix, we will evaluate the various generalized admittances appearing in (23) and (24).

First, we evaluate Y_{11}^{a1} given by

$$Y_{11}^{a1} = -\langle \boldsymbol{M}_{11}, \boldsymbol{H}_t^a(\boldsymbol{M}_{11})\rangle_1 = -\int_{-w_1}^{w_1} \boldsymbol{M}_{11}\cdot\boldsymbol{H}_t^a(\boldsymbol{M}_{11})\,dx'. \tag{A1}$$

Here, the integration is along the x direction in slot S_1 and $\boldsymbol{M}_{11}$ is given by

$$\boldsymbol{M}_{11} = -\frac{1}{\sqrt{w_1^2 - x^2}}\hat{y} \qquad \text{in } S_1. \tag{A2}$$

Also in (A1), $\boldsymbol{H}^a(\boldsymbol{M}_{11})$ is the magnetic field due to current $\boldsymbol{M}_{11}$ radiating in region a with slot S_1 closed. At observation point (x, z) in region a, this field is due to $2\boldsymbol{M}_{11}$ radiating in free space. That is

$$\boldsymbol{H}^a(\boldsymbol{M}_{11}) = -\frac{k_a}{2\eta_a}\int_{-w_1}^{w_1} \frac{1}{\sqrt{w_1^2 - x'^2}} \cdot H_0^{(2)}\left(k_a\sqrt{z^2 + (x-x')^2}\right) dx'\hat{y} \tag{A3}$$

where $H_0^{(2)}$ is the Hankel function of the second kind of zero order. In the slot S_1 region, the Hankel function can be replaced by its small argument approximation

$$H_0^{(2)}\left(k_a\sqrt{z^2 + (x-x')^2}\right)\Big|_{\substack{z=0 \\ x,x' \in [-w_1, w_1]}} \approx 1 - j\frac{2}{\pi}\log\frac{k_a\gamma|x-x'|}{2} + \cdots \tag{A4}$$

where log denotes natural logarithm and $\gamma = 1.7810724$. Substituting (A4) into (A3), employing the identities

$$\int_{-w}^{w} \frac{1}{\sqrt{w^2 - x'^2}}\, dx' = \pi \tag{A5}$$

$$\int_{-w}^{w} \frac{1}{\sqrt{w^2 - x'^2}} \log\frac{\gamma k|x-x'|}{2}\, dx' = \pi\log\left(\frac{\pi k w}{4}\right) \tag{A6}$$

and retaining only the largest real and imaginary terms, one readily obtains

$$\boldsymbol{H}^a(\boldsymbol{M}_{11}) = -\frac{k_a\pi}{2\eta_a}\hat{y} + j\frac{k_a}{\eta_a}\log\left(\frac{\gamma k_a w_1}{4}\right)\hat{y} \qquad \text{in } S_1. \tag{A7}$$

Note that $\boldsymbol{H}^a(\boldsymbol{M}_{11})$ is constant in the slot S_1 region. Finally, we substitute (A7) for $\boldsymbol{H}_t^a(\boldsymbol{M}_{11})$ in (A1) and readily arrive at

$$Y_{11}^{a1} = \frac{k_a\pi^2}{2\eta_a} - j\frac{k_a\pi}{\eta_a}\log\left(\frac{\gamma k_a w_1}{4}\right). \tag{A8}$$

Next, we evaluate Y_{11}^{b1} given by

$$Y_{11}^{b1} = -\langle \boldsymbol{M}_{11}, \boldsymbol{H}_t^b(\boldsymbol{M}_{11})\rangle_1 = -\int_{-w_1}^{w_1} \boldsymbol{M}_{11}\cdot\boldsymbol{H}_t^b(\boldsymbol{M}_{11})\, dx' \tag{A9}$$

where the integration is along the x direction in slot S_1 and $\boldsymbol{M}_{11}$ is given by (A2). Also in (A9), $\boldsymbol{H}^b(\boldsymbol{M}_{11})$ is the magnetic field due to the current $\boldsymbol{M}_{11}$ radiating in region b with both slots S_1 and S_2 closed. At observation point (x, z) in region b, this field is the field due to $2\boldsymbol{M}_{11}$ and its $2d$-spaced images. That is

$$\boldsymbol{H}^b(\boldsymbol{M}_{11}) = -\frac{k_b}{2\eta_b}\sum_{n=-\infty}^{\infty}\int_{-w_1}^{w_1} \frac{1}{\sqrt{w_1^2 - x'^2}} \cdot H_0^{(2)}\left(k_b\sqrt{(z-2nd)^2 + (x-x')^2}\right) dx'. \tag{A10}$$

In the slot S_1 region, the following approximations for the Hankel function are considered. For $n = 0$, $H_0^{(2)}$ is replaced by its small argument approximation

$$H_0^{(2)}\left(k_b\sqrt{z^2 + (x-x')^2}\right)\Big|_{\substack{z=0 \\ x,x' \in [-w_1, w_1]}} \approx 1 - j\frac{2}{\pi}\log\frac{k_b\gamma|x-x'|}{2} + \cdots. \tag{A11}$$

For $n^2 > (10w_1/d)^2$, we have $(2nd)^2 \gg |x-x'|^2$ and thus we can set

$$H_0^{(2)}\left(k_b\sqrt{(z-2nd)^2 + (x-x')^2}\right)\Big|_{\substack{z=0 \\ x',x \in [-w_1, w_1]}} \approx H_0^{(2)}(|2k_b nd|). \tag{A12}$$

Substituting (A11) and (A12) into (A10) and employing identities (A5) and (A6), we obtain

$$\begin{aligned}\boldsymbol{H}^b(\boldsymbol{M}_{11}) = &-\frac{k_b\pi}{2\eta_b}\hat{y} + j\frac{k_b}{\eta_b}\log\frac{\gamma k_b w_1}{4}\hat{y} \\ &-\frac{k_b}{\eta_b}\sum_{n=1}^{N_1}\int_{-w_1}^{w_1}\frac{1}{\sqrt{w_1^2 - x^{12}}} \cdot H_0^{(2)}\left(k_b\sqrt{(2nd)^2 + (x-x')^2}\right) dx' \\ &-\frac{k_b\pi}{\eta_b}\sum_{n=N_1+1}^{\infty} H_0^{(2)}(2k_b nd)\,\hat{y} \qquad \text{in } S_1\end{aligned} \tag{A13}$$

where N_1 is the largest integer n satisfying $n^2 \leqslant (10w/d)^2$, with w being $\max(w_1, w_2)$.

Finally, we substitute (A13) for $\boldsymbol{H}_t^b(\boldsymbol{M}_{11})$ in (A9) and readily arrive at

$$\begin{aligned}Y_{11}^{b1} = &\frac{k_b\pi^2}{2\eta_b} - j\frac{k_b\pi}{\eta_b}\log\left(\frac{\gamma k_b w_1}{4}\right) \\ &+\frac{k_b}{\eta_b}\sum_{n=1}^{N_1}\int_{-w_1}^{w_1}\int_{-w_1}^{w_1}\frac{1}{\sqrt{w_1^2 - x'^2}}\frac{1}{\sqrt{w_1^2 - x^2}} H_0^{(2)} \\ &\cdot\left(k_b\sqrt{(2nd)^2 + (x-x')^2}\right) dx'\,dx \\ &+\frac{k_b\pi^2}{\eta_b}\sum_{n=N_1+1}^{\infty} H_0^{(2)}(2k_b nd).\end{aligned} \tag{A14}$$

We now proceed to evaluate Y_{12}^{b1} given by

$$Y_{12}^{b1} = \langle \boldsymbol{M}_{11}, \boldsymbol{H}_t^b(\boldsymbol{M}_{21})\rangle_1 = \int_{-w_1}^{w_1} \boldsymbol{M}_{11}\cdot\boldsymbol{H}_t^b(\boldsymbol{M}_{21})\, dx' \tag{A15}$$

where the integration is along the x direction in slot S_1, and $\boldsymbol{M}_{11}$ is given by (A2). Also in (A15) $\boldsymbol{H}^b(\boldsymbol{M}_{21})$ is the

magnetic field due to the current

$$\boldsymbol{M}_{21} = \frac{1}{\sqrt{w_2^2 - (x - s_2)^2}} \qquad \text{in } S_2 \qquad \text{(A16)}$$

radiating in region b with both slots S_1 and S_2 closed. At observation point (x, z) in region b, this field is the field due to $2\boldsymbol{M}_{21}$ and its $2d$-spaced images. That is,

$$\boldsymbol{H}^b(\boldsymbol{M}_{21}) = -\frac{k_b}{2\eta_b} \sum_{n=-\infty}^{\infty} \int_{s_2 - w_2}^{s_2 + w_2} \frac{1}{\sqrt{w_2^2 - (x' - s_2)^2}} \cdot H_0^{(2)}\left(k_b \sqrt{[z - (2n-1)\,d]^2 + (x - x')^2}\right) dx'\,\hat{\boldsymbol{y}}. \qquad \text{(A17)}$$

In the slot S_1 region, the following approximation for the Hankel function is considered. For $(2n-1)^2 > (10w_2/d)^2$, we set

$$H_0^{(2)}\left(k_b \sqrt{[z - (2n-1)d]^2 + (x - x')^2}\right)\Big|_{\substack{z=0 \\ x \in [-w_1, w_1] \\ x' \in [s_2 - w_2, s_2 + w_2]}} \approx H_0^{(2)}\left(k_b \sqrt{[(2n-1)\,d]^2 + s_2^2}\right). \qquad \text{(A18)}$$

Substituting (A18) into (A17) and employing (A5), we find

$$\boldsymbol{H}^b(\boldsymbol{M}_{21}) = -\frac{k_b}{\eta_b} \sum_{n=1}^{N_2} \int_{s_2 - w_2}^{s_2 + w_2} \frac{1}{\sqrt{w_2^2 - (x' - s_2)^2}} \cdot H_0^{(2)}\left(k_b \sqrt{[z - (2n-1)\,d]^2 + (x - x')^2}\right) dx'\,\hat{\boldsymbol{y}} - \frac{k_b \pi}{\eta_b} \sum_{n=N_2+1}^{\infty} H_0^{(2)}\left(k_b \sqrt{[(2n-1)\,d]^2 + s_2^2}\right)\hat{\boldsymbol{y}} \qquad \text{in } S_1 \qquad \text{(A19)}$$

where N_2 is the largest integer n satisfying $(2n-1)^2 \leqslant (10w_2/d)^2$. Finally, we substitute (A19) for $\boldsymbol{H}_t^b(\boldsymbol{M}_{21})$ in (A15) and readily arrive at

$$Y_{12}^{b1} = -\frac{k_b}{\eta_b} \sum_{n=1}^{N_2} \int_{-w_1}^{w_1} \int_{s_2 - w_2}^{s_2 + w_2} \frac{1}{\sqrt{w_2^2 - (x' - s_2)^2}} \frac{1}{\sqrt{w_1^2 - x^2}} \cdot H_0^{(2)}\left(k_b \sqrt{[(2n-1)\,d]^2 + (x - x')^2}\right) dx'\,dx - \frac{k_b \pi^2}{\eta_b} \sum_{n=N_2+1}^{\infty} H_0^{(2)}\left(k_b \sqrt{[(2n-1)\,d]^2 + s_2^2}\right). \qquad \text{(A20)}$$

Furthermore, thanks to reciprocity,

$$Y_{21}^{b1} = Y_{12}^{b1}. \qquad \text{(A21)}$$

The remaining elements Y_{22}^{b1} and Y_{22}^{c1} can be evaluated in a way analogous to that used to evaluate Y_{11}^{b1} and Y_{11}^{a1}, respectively. The result is

$$Y_{22}^{b1} = \frac{k_b \pi^2}{2\eta_b} - j\frac{k_b \pi}{\eta_b} \log\left(\frac{\gamma k_b w_2}{4}\right) + \frac{k_b}{\eta_b} \sum_{n=1}^{N_1} \int_{-w_2}^{w_2} \int_{-w_2}^{w_2} \frac{1}{\sqrt{w_2^2 - x'^2}} \frac{1}{\sqrt{w_2^2 - x^2}} \cdot H_0^{(2)}\left(k_b \sqrt{(2nd)^2 + (x - x')^2}\right) dx'\,dx + \frac{k_b \pi^2}{\eta_b} \sum_{n=N_1+1}^{\infty} H_0^{(2)}(2k_b nd) \qquad \text{(A22)}$$

$$Y_{22}^{c1} = \frac{k_c \pi^2}{2\eta_c} - j\frac{k_c \pi}{\eta_c} \log\left(\frac{\gamma k_c w_2}{4}\right). \qquad \text{(A23)}$$

Acknowledgment

The author is pleased to acknowledge helpful discussions with Prof. A. Lewis and E. Betzig of Cornell University.

References

[1] C. M. Butler, Y. Rahmat-Samii, and R. Mittra, "Electromagnetic penetration through apertures in conducting surfaces," *IEEE Trans. Antennas Propagat.*, vol. AP-26, pp. 82–93, Jan. 1978.

[2] E. A. Ash and G. Nichols, "Super-resolution aperture scanning microscope," *Nature*, vol. 237, pp. 510–512, June 1972.

[3] A. Lewis *et al.*, "Development of a 500 angstrom spatial resolution light microscope," *Ultramicroscopy*, vol. 13, no. 3, pp. 227–232, 1984.

[4] D. T. Auckland and R. F. Harrington, "Electromagnetic transmission through a filled slit in a conducting plane of finite thickness, TE case," *IEEE Trans. Microwave Theory Tech.*, vol. MTT-26, pp. 499–505, July 1978.

[5] D. T. Auckland and R. F. Harrington, "A nonmodal formulation for electromagnetic transmission through a filled slot of arbitrary cross section in a thick conducting screen," *IEEE Trans. Microwave Theory Tech.*, vol. MTT-28, pp 548–555, June 1980.

[6] R. F. Harrington and D T. Auckland, "Electromagnetic transmission through narrow slots in thick conducting screens," *IEEE Trans. Antennas Propagat.*, vol. AP-28, pp. 616–622, Sept. 1980

[7] C. Cha and R. F. Harrington, "Electromagnetic transmission through a rotationally symmetric hole in a thick screen," Rep. TR-81-2, Dept. Electrical and Computer Engineering, Syracuse University, June 1981

[8] Y. Leviatan, R. F. Harrington, and J. R. Mautz, "Elecromagnetic transmission through apertures in a cavity in a thick conductor," *IEEE Trans. Antennas Propagat.*, vol AP-30, pp 1153–1165, Nov. 1982.

[9] R. F. Harrington, *Time-Harmonic Electromagnetic Fields*. New York: McGraw-Hill, 1961.

[10] R. F. Harrington, *Field Computation by Moment Methods*. New York: Macmillan, 1968

[11] R F. Harrington and J. R Mautz, "A generalized network formulation for aperture problems," *IEEE Trans. Antennas Propagat.*, vol AP-24, pp 870–873, Nov. 1976.

[12] C M. Butler and D. R. Wilton, "General analysis of narrow strips and slots," *IEEE Trans. Antennas Propagat.*, vol AP-28, pp. 42–48, Jan. 1980.

[13] Y. Leviatan, "Study of near-zone fields of a small aperture," *J. Appl Phys.*, vol 60, pp. 1577–1583, Sept. 1986.

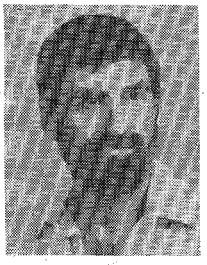

Yehuda Leviatan (S'81–M'82) was born in Jerusalem, Israel, on September 19, 1951. He received the B.Sc. and M.Sc. degrees in electrical engineering from the Technion—Israel Institute of Technology, Haifa, Israel, in 1977 and 1979, respectively, and the Ph.D. degree in electrical engineering from Syracuse University, Syracuse, NY, in 1982.

He held a Teaching Assistantship during his graduate work from 1977 to 1979 at the Technion, a Research Assistantship during his graduate work from 1979 to 1981 at Syracuse University, and a Postdoctoral Research position at Syracuse University during the summer of 1982. From 1980 to 1982 he was also engaged as a part-time Research Engineer at the Syracuse Research Corporation. During the 1982/83 academic year he was with the Faculty of the Electrical and Computer Engineering Department at Syracuse University as an Assistant Professor. He has provided consulting services to the Syracuse Research Corporation, IBM (Endicott Laboratory), and to Adaptive Technology, Inc. In October 1983 he joined the Department of Electrical Engineering at the Technion, where at present he is a Senior Lecturer. During the summer of 1985 he was a Visiting Assistant Professor with the School of Applied and Engineering Physics, Cornell University.

Dr. Leviatan's research interests are in the areas of mathematical and numerical methods applied to antennas, transmission lines, and waveguides, scattering and transmission through apertures, and near fields of radiating systems. He has published several journal papers on electromagnetics and presented others at international symposia. A paper he coauthored won the third best award at the 1983 IEEE International EMC Symposium. He is a Fellow of the B. De Rothschild Foundation for the Advancement of Science in Israel Inc., and a member of Commission E of the International Union of Radio Science.